Dynamics of the northern Portuguese shelf and related sediment transport processes

João Vitorino and Emanuel Coelho

Marinha - Instituto Hidrográfico
Rua das Trinas 49, P - 1296 Lisboa codex, Portugal

1. Introduction

In the last decade, several observational programs revealed the presence of fine sediment deposits over the mid-shelf off the northern Portuguese coast. One of those deposits - the Douro muddy complex (DMC) - by its extension and nature, has deserved special attention. This complex is found between the Douro river (41°N) to the Minho river (41°52'N), roughly following the 90-m isobath (Figure 1) and extending from the 65-m to the 130-m isobaths [Drago e*t al.*, 1998]. Both sedimentary and chemical evidences suggest that the fine sediments of DMC are provided by the Douro river, which is the most important river in this area [Araújo *et al.*, 1994]. Actual accumulation rates are estimated between 0.16 and 0.57 cm yr^{-1} [Cascalho and Ramos, 1990; Drago, 1995].

The presence of this deposit of fine sediments at the mid-shelf, with actual net deposition rates, indicates a low energy dynamics in this area, with the exception of some events of resuspension. Also, the fine sediments from DMC are only found northwards of the Douro river, tough as the probable source of sediments for the complex, which can suggest that the feeding of the DMC and/or the remobilization of sediments must occur during conditions characterized by northwards transport. This point was recently discussed by Drago *et al.* [1998]. They argued that the feeding of sediments to the DMC must occur mostly during winter and early spring, when river discharge is maximum, and that the downwelling regime that prevails during this period must lead to a gradual northwards and offshore displacement of the sediments in a succession of deposition and resuspension steps.

2. The observational program.

In the framework of OMEX II-II, the Instituto Hidrográfico (partner IH8a) has conducted an observational program on the northern Portuguese coast aiming to provide observational support to some of the hypothesis previously stated about the processes affecting the DMC. Two main objectives were envisaged:

a) to characterize the mid-shelf dynamics over the DMC at different time-scales (**Task II.1)**

b) to observe the combined effect of waves and currents on the remobilization and transport of the fine sediment of DMC (**Task III.1**).

The program started in the winter 1996, with a set of current-meter, wave and hydrographic observations. These were further extended during 1998, with long term wave and current-meter observations.

3. Data and methods

The observations discussed here include current-meter and wave measurements taken between 29 January and 15 May 1998 at the position 41°19'4"N, 8°58'54"W. The observational site is located over the mid-shelf off Leixões (bottom depth 86 m) and inside the region covered by the DMC (Figure 1). Its bathymetry is roughly aligned in the N-S direction but distorted at the outer shelf by the Porto Canyon.

Current-meter observations

A current-meter mooring equipped with 4 Aanderaa RCM-7 current-meters and 1 Aanderaa RCM-9 current-meter was deployed on 29 January 1998 (Table 1). Although this mooring has been damaged by mid-March, almost all the RCMs have been recovered and the inspection of the data has revealed that there were good measurements for periods covering 2.2 to 3.5 months.

Basic current meter data include current, temperature, pressure and conductivity measurements with a sampling rate of 20 minutes for all the observation depths. Note that two methodologies were used to measure the current, the RCM-7 measurements are based on a classical rotor system while the RCM-9 meter is based on Doppler effect.

In addition to these measurements, the RCM-9 current-meter was equipped with a turbidity sensor, which provided, every 20 minutes, a measure of the amount of suspended matter in the water at 6 m above the seafloor.

Having selected the periods of good data periods for each current-meter (Table 1) the data were filtered with a 2 hours low-pass Buttherworth filter and decimated to hourly intervals. Spectra (not show) of these hourly time series were used to define three frequency domains corresponding to different types of dominant processes. These are the low-frequency (subinertial) band, which corresponds to fluctuations with time scales longer than 28 hours, the inertial band that includes fluctuations with periods between 16 and 28 hours and the tidal band which corresponds to signals with time scales shorter than 16 hours and includes the dominant semi-diurnal M_2 tide. The time series corresponding to each of these frequency domains were obtained from the hourly original time series by filtering with an order-7 Buttherworth filter (respectively low-pass, band-pass and high pass). In all cases two days of data were removed from each end of the filtered time series.

The turbidity data from the RCM-9 meter were not filtered. The turbidity signal showed a marked degradation of the signal quality from about 7 March. This was calibrated by using the periods of apparent low energetic conditions to define linear fits, which were subsequently removed. The turbidity series was truncated at 25 April due to the poor quality of the signal after this date.

current-meter	type	valid period	depth
10972	RCM-7	29/1 - 14/4	23 m (63 mab)
10974	RCM-7	29/1 - 17/5	50 m (36 mab)
9601	RCM-7	29/1 - 10/5	70 m (16 mab)
77	RCM-9	29/1 - 17/5	80 m (6 mab)

Table 1. Description of current-meter measurements

Waves

Observations of waves for the same period of current-meter measurements were obtained from a directional WAVEC buoy located at the position of the current-meter mooring. This buoy is maintained at this location by IH since 1993. It measures the elevation and slope of the sea surface in north and east directions, during intervals of 20 minutes starting every 3 hours (or starting every 30 minutes if significant wave height exceeds 5 m). The data are then transmitted to a coastal station. Further details on the equipment's and data processing can be found in Anonymous [1994].

Wave data consists of wave spectral power estimates and directional spectra obtained with 6 degrees of freedom for 123 estimates with spectral resolution of df = 0.005 Hz. The periods covered range from 1.5 s to 40 s. Summary statistics (significant wave height Hs, mean period and peak period) are also derived.

From the wave spectra we have calculated the spectra of wave orbital velocity at the bottom. Then a significant wave orbital velocity at the bottom was estimated, in analogy with the definition of significant wave height. The directions of the waves that correspond to the peak of the wave orbital velocity spectra were obtained from the directional spectra. Using the significant orbital velocity at the bottom, and assuming a laminar oscillatory boundary layer over a smooth, flat bottom, the shear velocity induced by waves was then estimated.

Meteorology

No direct meteorological measurements were conducted during the period of current observations. ECMWF daily winds at a position close to the mooring site (40°56'N, 9°00'W), obtained from BADC, were used as the representative wind conditions on the study area for the period of observations.

4. Mid-shelf dynamics off northern Portugal - January to May 1998 (**Task II.1**).

The current measurements were undertaken during typical winter conditions, with southerly winds persisting for at least one month, from the end of January until the first week of March (Figure 2). In accordance with this downwelling favorable wind forcing, a poleward residual flow was observed at all levels over the mid-shelf. At the two uppermost levels this flow shows an onshore component (reflecting onshore transport in the upper Ekman layer) while at the two deepest levels it has an offshore component (which could reflect the interaction of the poleward flow with the lower Ekman layer). During this period, and as the result of previous episodes of strong mixing, the water column was rather homothermic with temperatures at all levels around 15°C. Weak stratification effects were restricted to the uppermost levels where the influence of the Douro river plume is sometimes apparent in the salinity time series (not show). At the same time a gradual increase of salinity was observed at levels below 23 m.

The conditions previously described remained remarkably constant until mid-March, despite the occurrence of a moderate upwelling event, by the end of February, which drives an equatorward jet of 20 cm s^{-1} (Figure 2). This situation radically changes by mid-March when a strong upwelling event was observed. In response to the establishment of sustained northerly winds during a week, a strong barotropic equatorward jet was established over the mid-shelf with currents as strong as 45 cm s^{-1} being measured at all levels until 6 m above the bottom. The jet veers from offshore oriented at the shallowest level to onshore oriented at the two deepest level, which must reflect the fact that measurements extended from the surface Ekman layer, were offshore transport is expected, through the interior and reached the bottom Ekman layer where onshore compensatory transport must occur. It is noteworthy that onshore flow at 80 m (6 m above the bottom) reaches 20 cm s^{-1} during this event.

This upwelling event, contrarily to the one observed previously, had a profound impact on the hydrographic conditions over the mid-shelf. The inspection of the temperature and salinity (not show) time series revealed that as the strong upwelling jet develops, cold and less saline water progressively appears at the deepest levels over the mid shelf. A decrease of about 1°C occurred in 3 days at 80 m depth, while at the upper levels this decrease was more gradual. By the end of the event, one week after, the temperature has fallen by 1°C at all observation levels. This behavior tend to suggest that the cross-shore circulation associated with this upwelling event was able to promote a rapid advection of waters from deeper levels over the upper slope to the mid-shelf. The importance of the Porto canyon in this process is worth to be further discussed.

After that week, the winds return to southerly directed and poleward flow was again reestablished. This flow advects warm water (and probably also salt water although the salinity signal was no longer available by this time due to degradation of the conductivity cells) at the surface levels, promoting the establishment of some thermal stratification over the mid-shelf. By 2-3 April a strong storm occurred (see also Figure 4b) and the strong vertical mixing associated with this events completely homogenized the water column. It is interesting to note that after this period the temperature time series returned to the values that were observed prior to the upwelling event.

After 1 April, winds changed to northerly directed and remained so for a month. Under these upwelling favorable conditions a persistent equatorward flow occurred at all levels and a systematic fall of temperature was observed at the mid and lower water column (note that the 23-m signal was not longer available at this period). By the end of the observational period, temperature at these levels reached 12.5°C.

Just before the end of the observation period a 3-4 days event of southerly winds was able to completely reverse the flow pattern and drive a poleward flow over the mid-shelf as strong as 30 cm s^{-1} near the bottom.

Superimposed on the residual flow, the observations also reveal to presence of inertial and tidal motions. Several events of intensified inertial motions, in clear associated with the wind events, are shown in the time series presented in Figure 3. Inertial currents over the mid-shelf do not exceed 10 cm s^{-1} and are very isotropic. Tidal motions are dominated by the semi-diurnal (M_2) signal and are intensified and polarized in the cross-shore direction near the bottom. This polarization, also observed on the 1996 current-meter data, can reflect a guiding effect of the Porto canyon topography, which is located just offshore of the mooring site.

Despite the fact that the magnitude of inertial and tidal motions hardly exceed 10 cm s^{-1} and are much weaker than the magnitude of subinertial motions, they made a comparable contribution to the cross-shore circulation, since the residual flow is polarized in the along-shore direction (Table 2). This result is particularly true for the tidal motions, which are polarized in the cross-shore direction.

Depth (m)	block	extension (days)	U ± st.dev. (cm s^{-1})	% var. u	V ± st.dev. (cm s^{-1})	% var. v	Pdir. (degrees)
23	1	30	0.4 ± 1.9	39%	3.9 ± 4.8	77%	85
	2	30	0.4 ± 2.7	54%	-0.9 ± 9.1	94%	77
	3	12	-0.5 ± 2.4	31%	-3.3 ± 7.8	81%	75
	total	72	0.2 ± 2.4	44%	0.6 ± 8.0	81%	78
50	1	30	1.2 ± 2.2	52%	2.2 ± 4.9	77%	70
	2	30	0.8 ± 2.7	54%	-1.8 ± 10.8	94%	78
	3	30	0.0 ± 2.2	32%	-3.0 ± 7.8	82%	77
	4	17	-0.2 ± 3.7	52%	-6.1 ± 12.9	91%	76
	total	107	0.5 ± 2.7	47%	-1.6 ± 9.4	91%	77
70	1	30	0.5 ± 2.3	41%	1.5 ± 6.2	82%	87
	2	30	1.3 ± 3.1	51%	-2.0 ± 11.1	94%	102
	3	30	0.0 ± 1.7	14%	-3.8 ± 10.1	86%	92
	total	90	0.8 ± 2.6	36%	-2.6 ± 10.3	93%	97
80	1	30	0.1 ± 3.8	51%	1.3 ± 6.6	84%	102
	2	30	1.7 ± 5.6	73%	-2.5 ± 9.3	94%	119
	3	30	0.4 ± 3.9	43%	-3.2 ± 8.8	84%	111
	4	17	1.4 ± 6.0	61%	-5.0 ± 13.5	94%	112
	total	107	0.8 ± 4.8	58%	-2.0 ± 9.6	92%	112

Table 2. Basic statistics for the east-west (u) and north-south (v) components of residual currents. These include mean ± standard deviation, percentage of total variance contained in the low-frequency signals (% var), principal direction counted counterclockwise from east (Pdir). Both statistics for blocks of one month and the total length of the series are presented.

5. Physical processes affecting fine sediment remobilization and transport (**Task III.1**).

From 29 January to 20 April the turbidity measurements clearly reveal several periods of 2-3 days of increased amount of suspended matter 6 m above the bottom (Figure 4a). The close matching that exists between those events and the periods of energetic wave regime indicates that they correspond to resuspension events promoted by the wave action at the bottom. Using both turbidity and wave measurements at least 17 events can be identified for this period and these are indicated on Figure 4.

During the first two months of observations, the wave regime was consistent with the typical winter conditions observed off the northern Portuguese coast. The most energetic conditions observed correspond to periods of southerly winds with waves with significant wave heights of 4-5 m directed from northwest and a small contribution of the short term (periods lower than 8 s) components. These conditions are very frequent on this area and correspond to waves generated by fetches at higher latitudes on the Northern Atlantic that then latter propagate to the western Iberian coast [Pires, 1985; Anonymous, 1994].

A different type of conditions, also common during the winter, has occurred at the beginning of these observations (event 1). This corresponded to a period of southeasterly winds with waves coming from southwest. This type of conditions are usually established by quasi-steady lows centered southwest of the Iberian Peninsula or, on shorter periods, by the passage of cold fronts over the area [Pires, 1985].

With a single exception, all the turbidity events depicted in Figure 4a for these first two months of measurements corresponded to periods during which significant wave heights reached 4 m and the corresponding wave orbital velocity at the bottom and shear velocity exceeded respectively 25 cm s^{-1} and 0.8 cm s^{-1}. These events occurred during periods of poleward flow over the mid-shelf, associated with downwelling conditions.

Event 7 is an exception to what was previously referred, since relatively weak orbital and shear velocities were observed at this time. However this event occurred during the period of strong equatorward flow associated with the upwelling event referred in the previous section. This suggests that the strong flow was enable to promote fine sediment resuspension in somewhat moderate wave conditions.

The last period of one month for which turbidity measurements were available was characterized by extreme conditions. Two major storms occurred by the 2-3 April and 25-27 April. They lead to a regime of waves directed from northwest, with significant wave heights exceeding 6 m and periods over 15 s. During these two extreme events, orbital velocities at the bottom were estimated to be up to 45-50 cm s^{-1} and the corresponding shear velocities were stronger than 1.6 cm s^{-1}. Between these two storms the conditions remained highly energetic, leading to high values of turbidity above the bottom that persisted for almost two weeks.

The two storms observed during this period are typical of the extreme conditions found in the northwestern Iberian region. They are normally associated with generation areas in the northern Atlantic, moving rapidly eastwards [Pires, 1985; Anonymous, 1994].

6. Conclusions

The observations conducted in 1998 covered the end of the winter regime and the transition to the summer upwelling regime. In that aspect they can be seen as a set of observations complementary to the ones made in the winter 1996, which covered the transition to the winter regime. The 1998 measurements also covered different aspects of the wave regime during winter and transition periods.

The observations revealed that during the winter, resuspension events are generally associated with downwelling conditions and poleward flow over the mid-shelf. These conditions promote the transport of the fine sediment from the DMC, both northwards and offshore of the resuspension site, to regions were they can be less affected by waves and deposition can be more permanent.

Resuspension events that occur during upwelling conditions and strong southward jets have also been observed during two occasions (events 7 and 12). Although these events can promote an effective southwards transport of resuspended fine sediments from the DMC, they are also associated with onshore transport near the bottom. As a consequence of this, the fine sediments are exported to shallows regions were they are more affected by the waves and where a permanent deposition is no longer possible. The observations discussed here seem then to support the hypothesis invoked by Drago *et al.* [1998] to explain the extension of the DMC northwards from its source.

The 1998 data indicates that the resuspension of fine sediments from the DMC occurred whenever the shear velocity associated with the waves exceeded 0.8 cm s^{-1}. An abrupt increased in the amount of suspended matter 6 m above the bottom was observed when the shear velocity exceed 1.2 cm s^{-1} during storm events. These values seem to be in good accordance with the value of the critical shear velocity of 1 cm s^{-1} indicated by J.M. Jouanneau (pers. comm.) for the same area.

References

Anonymous (1994). Final report of sub-project A: "Wave climatology of the Portuguese coast". NATO PO-WAVES, 6/94-A, 80 p.

Araújo, M.F., J.M.A Dias, J.-M. Jouanneau (1994). Chemical characterization of the main sedimentary deposit at the north-western Portuguese shelf, *Gaia*, 9, 59-65.

Cascalho F.P and L.A. Ramos (1990). Lead 210 chronology in marine sediments from the northern continental margin of Portugal, in Actas do II Congr. Qual. Amb., Lisbon, pp A143-A151.

Drago, T. (1995). La vasière Ouest-Douro sur la plate-forme continentale nord-portugaise. Rôle, fonctionnement, évolution, Ph. D. Thesis, Univ. Bordeaux I, 265 p. (unpublished)

Drago, T., A. Oliveira, F. Magalhães, J. Cascalho, J.M. Jouanneau and J. Vitorino (1998). Some evidences of the northward fine sediment transport in the northern Portuguese continental shelf. *Oceanologica Acta*, 21, 2, 223-231.

Pires, H.O. (1985). Alguns aspectos do clima de agitação marítima de interesse para a navegação na costa de Portugal. O clima de Portugal, 37, 34 p.

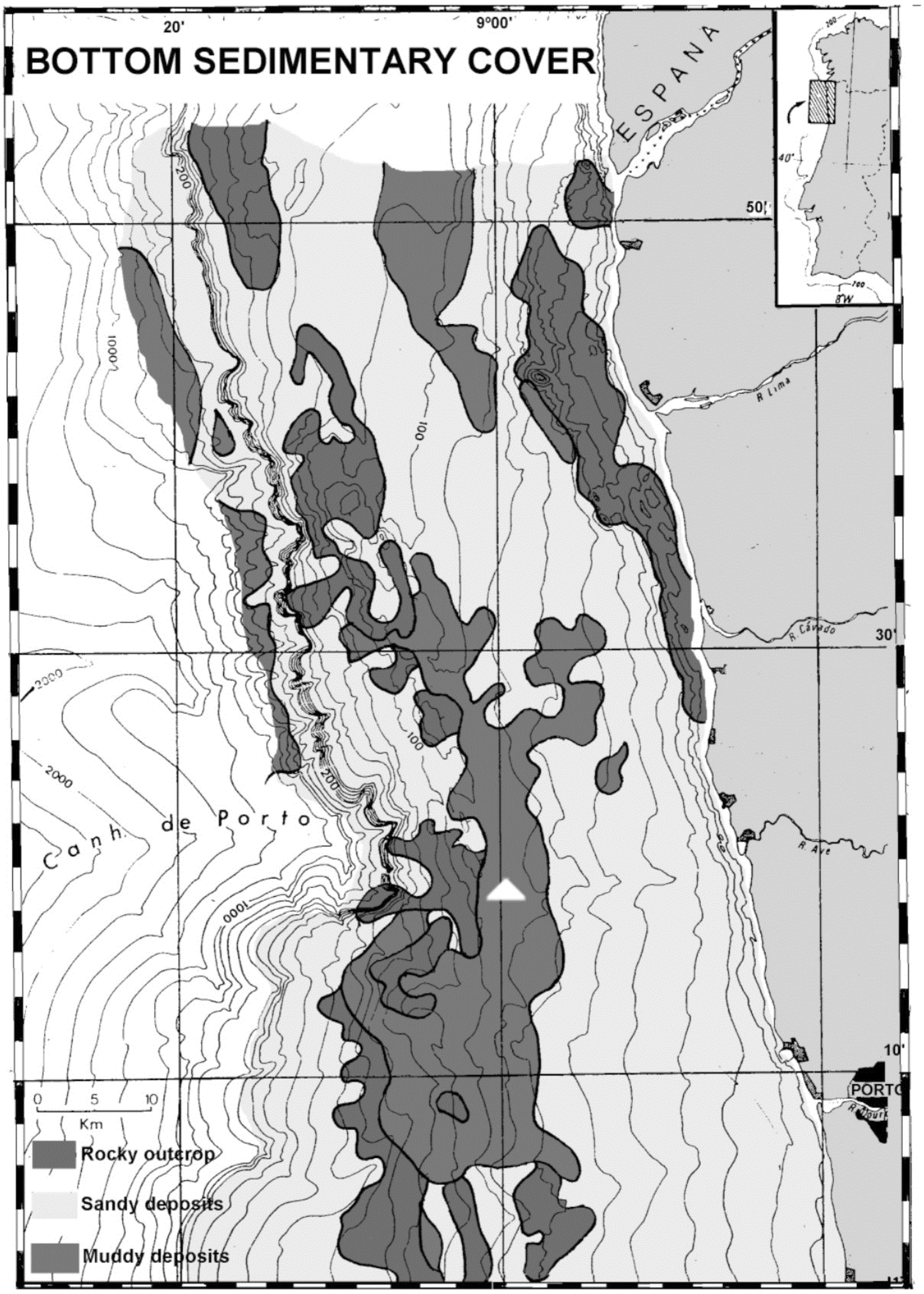

Figure 1. Bathymetry and sedimentary cover of the study area. The white triangle marks the location of current-meter mooring and wave buoy.

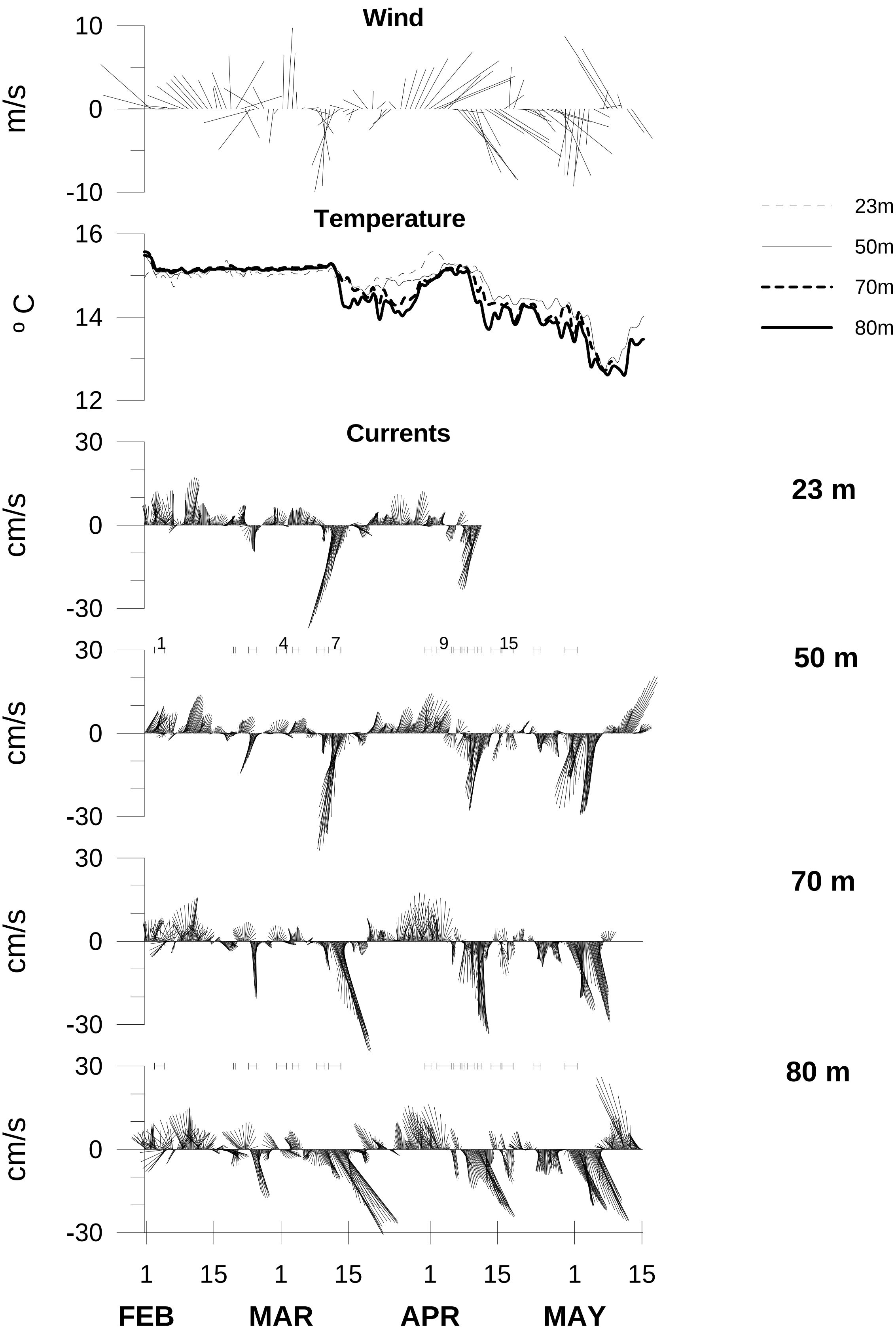

Figure 2. ECMWF winds near the mooring site, subinertial time series of temperature and currents at observational depths. Resuspension events are identified in the Figure.

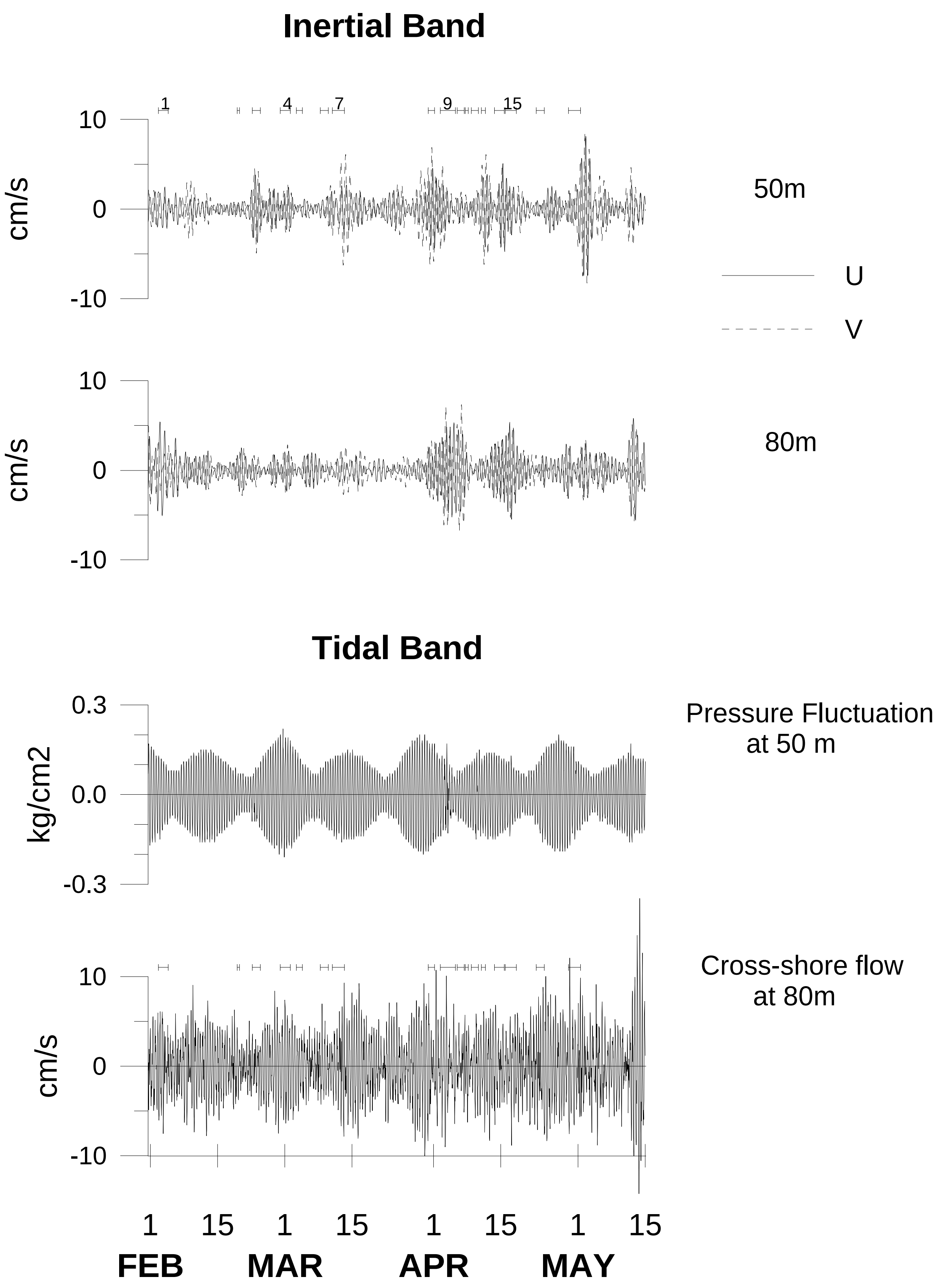

Figure 3. Time series of inertial currents, tidal pressure fluctuations at 50 m and cross-shore tidal flow at 80 m.

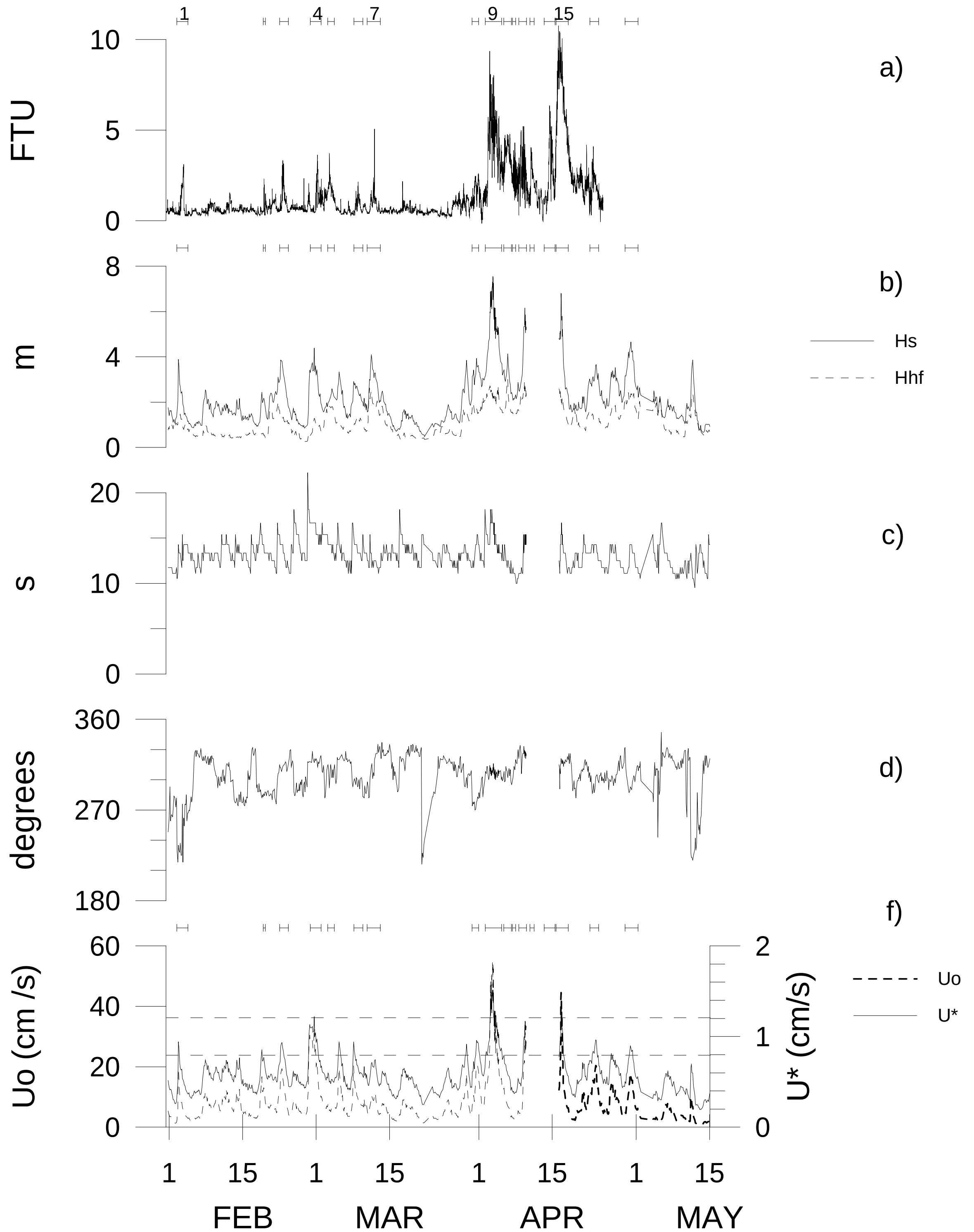

Figure 4. Time series of a) turbidity at 80 m depth (6 m above the bottom); b) significant wave height (Hs) and contribution of short term (T< 8 s) components (Hhf); Period c) and direction d) of waves corresponding to the peak of the orbital velocity spectrum; f) significant orbital velocity at the bottom (u_o) and estimated shear velocity (u_*).